PHYSICAL REVIEW A **82**, 020701(R) (2010)

# Giant Feshbach resonances in $^6$Li-$^{85}$Rb mixtures

B. Deh, W. Gunton, B. G. Klappauf, Z. Li, M. Semczuk, J. Van Dongen, and K. W. Madison
*Department of Physics and Astronomy, University of British Columbia, Vancouver, V6T 1Z1 Canada*
(Received 30 June 2010; published 10 August 2010)

We report on the observation of six large Feshbach resonances in a Fermi-Bose mixture of $^6$Li and $^{85}$Rb atoms. Near the resonances, both the elastic and inelastic collision rates are enhanced, and this results primarily in the loss of $^6$Li from an optical dipole trap since it is less massive and less confined than its $^{85}$Rb collision partner. We interpret our experimental data using a coupled-channels calculation which fully characterizes the ground-state scattering properties in any combination of spin states.

DOI: 10.1103/PhysRevA.82.020701 PACS number(s): 34.50.−s, 34.20.−b, 67.85.Pq

The field of ultracold atomic gases has been greatly enriched by the discovery and use of Feshbach resonances (FRs) [1]. FRs provide exquisite control over the microscopic interactions in atomic gases, and this control has been used to realize whole new classes of quantum many-body systems with tunable interactions [1]. In particular, FRs have revolutionized the study of pairing phenomena. FRs have enabled detailed studies of Bardeen-Cooper-Schrieffer (BCS) superfluid pairing and BEC-BCS crossover phenomena in two-component Fermi gases with both balanced and unbalanced populations [2–5]. Studying pairing in mass-imbalanced heteronuclear fermionic mixtures is now a possibility because broad FRs exist in $^6$Li-$^{40}$K mixtures [6,7]. Novel quantum phases [8–10] and pairing phenomena [11–14] in Fermi-Bose mixtures near narrow and broad FRs have also been considered theoretically. However, observing some of these proposed phenomena may prove to be technically more difficult because three-body inelastic losses are not as suppressed as in pure Fermi mixtures [1]. Mashayekhi *et al.* predicted that a mass-imbalanced Fermi-Bose mixture near a broad FR will undergo a first-order phase transition to a fully paired mixture when the scattering length exceeds a critical value. The critical scattering length at which this phase transition occurs was found to decrease with increasing boson-to-fermion mass ratio ($m_b/m_f$). The large mass ratio in Li-Rb mixtures may enable an experimental study of this phenomenon sufficiently far from a broad resonance that three-body inelastic losses are not a practical limitation. In addition, a large mass ratio can enhance the observability and study of Efimov-related physics in mass-imbalanced atomic mixtures [15]. FRs can also be used to create ultracold molecules by coherently linking ultracold atoms [1,16–18]. A primary motivation to form ground-state heteronuclear alkali dimers is that many possess a relatively large electric dipole moment (4.2 D for LiRb [19]), providing a route to studying a quantum gas with large, tunable, and anisotropic electric dipole-dipole interactions [20]. Another consequence of an electric dipole moment is that FRs can be induced and controlled in heteronuclear atomic mixtures by applying a static electric field which couples to the instantaneous dipole moment of the heteronuclear collision complex [21–23]. FRs can also be used to enhance evaporative cooling of atomic gases, and the resonances reported here may provide a way to efficiently cool $^{85}$Rb sympathetically with $^6$Li.

In this work, we experimentally observe six heteronuclear Feshbach resonances in a mixture of $^6$Li and $^{85}$Rb. We interpret the experimental data using a coupled-channels calculation, which allows us to predict the the ground-state scattering properties in any combination of spin states. We then use our calculations to identify and characterize seven broad resonances in $^6$Li-$^{85}$Rb and $^6$Li-$^{87}$Rb mixtures which are at experimentally convenient magnetic fields and are for states stable against spin exchange. The FR spectrum also offers an extremely sensitive probe of the least bound states of the interatomic interaction potentials. This work, combined with other recent experimental and theoretical work on the Li-Rb complex, makes it one of the best understood heteronuclear alkali systems [24–28]. This work provides data for further refinement of the interatomic potentials.

Our dual species magneto-optic trapping (MOT) apparatus is described in [29]. For these FR measurements, we load a $^6$Li MOT of $10^6$ atoms directly from an effusive oven. We then compress and cool the MOT by increasing the MOT axial magnetic field gradient from 40 to 60 G cm$^{-1}$, lowering the intensity and shifting the frequency of the trapping light from 35 to 10 MHz below resonance. During this cooling phase, a crossed dipole trap (CDT) is turned on, and in less than 10 ms, 10% of the $^6$Li atoms are transferred into the CDT. We observe trap losses due to light assisted collisions and hyperfine relaxation, and we therefore optically pump to the lower hyperfine state ($F = 1/2$) during the transfer. The light for the CDT is from a fiber laser (SP-100C-0013) operating at 1090 nm. Two beams, each with a maximum of 20 W (for a 40-W total CDT), are focused to a waist of 42 $\mu$m and 49 $\mu$m, crossing at an angle of 14°. The CDT is then ramped down to 15 W (7.5 W per beam) in 200 ms while applying a homogenous magnetic field of 840 G. This magnetic field is chosen close to the $^6$Li FR at 860 G to achieve rapid thermalization and efficient evaporation. At the end of this forced evaporation stage, there are approximately $5 \times 10^4$ atoms remaining. While holding $^6$Li in the CDT, we extinguish the homogenous field, turn on a magnetic quadrupole field, and, in 300 ms, load $10^5$ $^{85}$Rb atoms in a MOT from a background vapor. The atoms are transferred into the 15-W CDT by shifting the zero of the MOT magnetic quadrupole field to position the atom cloud at the crossing. Losses of both species ensue during this transfer (primarily light-assisted collisional losses; see [29]), and after the Rb MOT light is extinguished, the CDT contains approximately $2 \times 10^4$ of both $^6$Li and $^{85}$Rb atoms.

The trap oscillation frequencies in the 15-W CDT (7.5 W per beam) were characterized by parametric excitation [30], and for $^{85}$Rb ($^6$Li) they are 1500 Hz (3700 Hz) and 185 Hz

 

(453 Hz) in the radial and longitudinal directions respectively. The trap depths are $U_{\mathrm{Rb}}/k_{\mathrm{B}} = 471\ \mu$K and $U_{\mathrm{Li}}/k_{\mathrm{B}} = 196\ \mu$K. With both species loaded into the 15-W CDT, the temperatures, measured by the *in situ* size and a time-of-flight expansion, were approximately 150 $\mu$K for $^{85}$Rb and 70 $\mu$K for $^{6}$Li.

Our trapping laser has a line width exceeding 1 nm, and we observe that it drives two-photon stimulated Raman transitions between the $F = 2$ and $F = 3$ ground hyperfine states of $^{85}$Rb, while no such effect is observed for $^{6}$Li. To keep the Rb population in the lowest hyperfine state, we apply a weak beam of light tuned near the $5\,^2S_{1/2}, F = 3 \rightarrow 5\,^2P_{3/2}, F' = 2$ transition. As a result, our spin-state preparation degrades over time; nevertheless, we are able to greatly suppress the stretched spin states when required.

To detect FRs, we perform a second evaporative ramp of the CDT from 15 to 11 W in 500 ms while applying a homogenous magnetic field. After the ramp, the magnetic field is extinguished, the CDT is turned off, and we take an absorption image of either $^{6}$Li or $^{85}$Rb. During this ramp, cross-species thermalization and, for unstable spin mixtures, two-body spin relaxation result predominantly in the loss of $^{6}$Li from the CDT. In fact, we do not observe any discernible loss of $^{85}$Rb. This is because a $^{6}$Li atom is less deeply confined and less massive than $^{85}$Rb. Figure 1 shows the variation in the final $^{6}$Li atom number due to the presence of $^{85}$Rb as a function of the magnetic field. The data presented are for a mixture with some population in each of the ten spin states in the lowest hyperfine manifold ($|F = 2; m_F = -2, -1, 0, 1, 2\rangle_{^{85}\mathrm{Rb}} \otimes |F = 1/2; m_F = -1/2, +1/2\rangle_{^{6}\mathrm{Li}}$). Guided by our previous theoretical analysis of FRs in $^{6}$Li-$^{87}$Rb mixtures [27], we predicted a range of magnetic fields (from 300 to 1000 G) where none of the FRs in the ten spin states were overlapping and chose to search for loss features there. In order to verify that the features we observe are due to FRs between $^{6}$Li and $^{85}$Rb, an identical experimental run was performed, except that no Rb atoms are transferred from the MOT to the CDT. The $^{6}$Li atom number shown is normalized to the number observed when no $^{85}$Rb is transferred into the CDT. More than 50% of the Li atoms are lost during the transfer of Rb atoms into the CDT due to light-assisted collisions [29]. Additional losses of Li occur during the evaporation stage and depend on the magnetic field value. There are six resonance loss features visible in the data of Fig. 1. The loss features at 394 and 402 G arise from a pair of resonances between $^{85}$Rb atoms in the $|2,1\rangle$ state and $^{6}$Li in the $|\frac{1}{2}, \pm\frac{1}{2}\rangle$ states respectively. Likewise, the loss features at 315 and 466 G (950 and 975) arise from a pair of resonances between $^{85}$Rb atoms in the $|2,-2\rangle$ ($|2,-1\rangle$) state and $^{6}$Li in the $|\frac{1}{2}, \pm\frac{1}{2}\rangle$ states respectively.

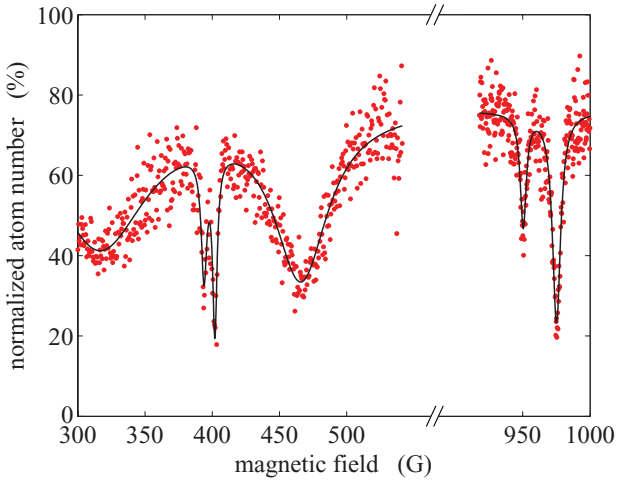


FIG. 1. (Color online) Normalized $^{6}$Li atom number after an evaporation ramp with $^{85}$Rb present as a function of magnetic field. All ten spin states in the lowest hyperfine manifold were populated. The dots are individual experimental runs, and the solid lines are fits of the resonance loss features to a sum of Gaussian functions. Cross-species thermalization and, for unstable spin mixtures, two-body spin relaxation leads to lithium atom loss. No $^{6}$Li-$^{85}$Rb FRs were apparent between 600 and 900 G, and from 50 to 250 G there was a broad loss feature due to multiple, overlapping FRs.

The minimum $^{6}$Li atom number for each resonance loss feature is not zero but rather a finite fraction of the initial number at the beginning of the second evaporative ramp. We assume this is, in part, because the $^{6}$Li population is distributed between the two magnetic sublevels in the lower hyperfine state, and the loss of both spin states would require thermalization collisions within the $^{6}$Li gas to exceed the collision rate between the $^{6}$Li and $^{85}$Rb atoms.

The positions and widths of the experimentally observed loss features are given in Table I. We calibrate the magnetic field up to 700 G with an uncertainty of 0.1% using microwave transitions between the two ground states of $^{85}$Rb. For higher magnetic fields, due to technical limitations, our determination of the field is less precise, and we therefore provide larger uncertainties on the resonance positions above 700 G. The theoretically predicted FR positions and an estimate of the expected widths of the loss features are also provided. The loss of atoms from the CDT is a dynamical process, and without a simulation of the ensemble dynamics during the evaporation ramp including the two- and three-body elastic and

TABLE I. Experimentally measured loss features associated with $s$-wave FRs for $^{6}$Li-$^{85}$Rb. The experimentally determined width $\Delta_{\mathrm{exp}}$ is the full width at half maximum of the trap-loss feature. The uncertainty in the measured positions ($B_0$) is a quadrature sum of the uncertainty in the fit to the experimental data and the uncertainty in the magnetic field. The theoretically predicted positions and estimated widths, $\Delta_{\mathrm{thy}}$, are derived from the $s$-wave elastic cross section obtained from a full coupled-channels calculation at a collision energy of $10^{-8}\mathrm{cm}^{-1}$.

| Atomic states | | Theory | | Experiment | |
|---|---|---|---|---|---|
| $\lvert f, m_f\rangle_{^{6}\mathrm{Li}}$ | $\lvert f, m_f\rangle_{^{85}\mathrm{Rb}}$ | $B_0$ (G) | $\Delta_{\mathrm{thy}}$ (G) | $B_0$ (G) | $\Delta_{\mathrm{exp}}$ (G) |
| $\lvert\frac{1}{2},\frac{1}{2}\rangle$ | $\lvert 2,-2\rangle$ | 312.1 | 60.8 | 315.4(5.8) | 65.2(5.8) |
| $\lvert\frac{1}{2},-\frac{1}{2}\rangle$ | $\lvert 2,-2\rangle$ | 466.7 | 47.0 | 466.4(3.6) | 47(3.5) |
| $\lvert\frac{1}{2},\frac{1}{2}\rangle$ | $\lvert 2,1\rangle$ | 393.0 | 5.1 | 393.9(0.8) | 3.92(0.29) |
| $\lvert\frac{1}{2},-\frac{1}{2}\rangle$ | $\lvert 2,1\rangle$ | 402.5 | 3.2 | 401.9(0.8) | 4.24(0.32) |
| $\lvert\frac{1}{2},\frac{1}{2}\rangle$ | $\lvert 2,-1\rangle$ | 937.7 | 7.1 | 950.5(9.1) | 6.32(0.47) |
| $\lvert\frac{1}{2},-\frac{1}{2}\rangle$ | $\lvert 2,-1\rangle$ | 961.3 | 7.2 | 975(10) | 7.28(0.55) |

inelastic collision cross sections, the width of the loss features cannot be predicted in a quantitative way. Nevertheless, we provide a qualitative estimate for the expected width from the theoretically computed $s$-wave elastic cross section, $\sigma_{\rm el}$, based on the assumption that the Li loss rate due to Li-Rb collisions, and therefore the loss feature shape, is proportional to $\sigma_{\rm el}$. This assumption neglects, among other things, saturation effects discussed earlier. To deduce the expected widths, we first observe that $\sigma_{\rm el} > 3.62 \times 10^5 a_0$ in a 47-G-wide region from 442.8 to 489.8 G, corresponding to the half width of the experimentally observed loss feature at 466.4 G. We then report the width of the magnetic field ranges in which $\sigma_{\rm el}$ exceeds this threshold for each of the other five FRs in Table I. The expected widths estimated in this qualitative way are in reasonable agreement with the experimentally measured values.

Our analysis of the data is based on our previous analysis of FRs in $^6$Li-$^{87}$Rb mixtures [27]. We use the model triplet $a\,^3\Sigma$ and singlet $X\,^1\Sigma$ interaction potentials of LiRb that we determined previously. These potentials correctly reproduced the experimentally measured FR spectrum of $^6$Li-$^{87}$Rb mixtures and were adjusted to reproduce the overall shape expected from the *ab initio* potential calculations for LiRb [19] and the number of bound states for the LiRb dimer determined from Fourier transform spectroscopy performed in the group of Tiemann and reported in [28]. The van der Waals coefficients were also taken from that work [28]: $C_6 = 2550.0 E_H\, a_{\rm B}^6$ and $C_8 = 2.3416 \times 10^5 E_H\, a_{\rm B}^8$ (where the Bohr radius is $a_{\rm B} = 0.529 \times 10^{-10}$ m and $E_H = 4.35974 \times 10^{-18}$ J).

We first used these potentials in a full coupled-channels scattering calculation to compute both the $s$- and $p$-wave elastic collision cross sections as a function of the magnetic field for a distribution of collision energies corresponding to the temperature in our experiment (150 $\mu$K). Based on our previous analysis of $^6$Li-$^{87}$Rb mixtures, we chose not to include dipole-dipole interactions in these calculations as they produce negligibly small shifts to the FR spectrum. More details of our calculation methods are described in [27]. Our calculations provided a FR spectrum for the $^6$Li-$^{85}$Rb mixture for the each of the ten spin states in the lowest hyperfine manifold. The agreement between the experimental and theoretical FR spectra was initially good, but the resonance locations were not in perfect agreement. By optically pumping our $^{85}$Rb sample to eliminate population in particular spin states, we were able to eliminate the corresponding loss features and thus verify the spin-state assignment of the FRs. With this information in hand, we proceeded to fine-tune our potentials to match as well as possible the experimentally measured locations of the six distinct FRs. Since the long-range behavior of the potentials is well known, the potentials could only be refined by making small adjustments to the short-range repulsive wall while keeping the long-range behavior fixed. To simplify the search, we employed the asymptotic bound-state model (ABM) to first determine the energies of the least bound states of the triplet and singlet potentials consistent with the experimentally observed location of the FRs. Details of the model and how this search is done are described in [27]. We then adjusted the potential curves to reproduce these bound-state energies. With these updated potentials, we computed the locations and widths of the FRs using the full coupled-channels scattering calculation and made final refinements to reproduce as closely as possible the location and widths of the experimentally observed Feshbach resonances. For the optimal singlet and triplet potentials, the energies of the least bound states are $E_{\rm singlet} = -0.09669$ cm$^{-1}$ and $E_{\rm triplet} = -0.1312$ cm$^{-1}$. The calculated singlet and triplet scattering lengths are 8.87 and $-14.88 a_{\rm B}$ respectively. These values are similar to, but not in perfect agreement with, those inferred for this isotope combination from an analysis of FRs in $^6$Li-$^{87}$Rb and $^7$Li-$^{87}$Rb mixtures [28].

The $s$-wave scattering length near a FR has the form $a(B) = a_{\rm bg}(1 - \Delta B/(B - B_0))$, where $a_{\rm bg}$ is the background scattering length, $B_0$ is the position, and $\Delta B$ is the width of the resonance [1]. The strength of a FR can be characterized by an effective length scale $r_{\rm e} = \hbar^2/(2m_{\rm R}|a_{\rm bg}|\mu_{\rm rel}\Delta B)$ and corresponding energy scale $E_{\rm res} = \hbar^2/(2m_{\rm R}r_{\rm e}^2)$, where $m_{\rm R}$ is

TABLE II. The calculated characteristics of seven large FRs for stable Fermi-Bose mixtures of $^6$Li-$^{85}$Rb and $^6$Li-$^{87}$Rb. The background scattering length $a_{\rm bg}$ and effective range of the resonance $r_{\rm e}$ are given in units of the Bohr radius, $a_0$. The value for $\mu_{\rm rel}$, the difference in the magnetic moments of the closed channel (molecule) and the open-channel threshold, is given in units of the Bohr magneton $\mu_{\rm B} = 9.27400915(23)$ J T$^{-1}$. For each FR, the magnetic fields at which the mixture is energetically stable with respect to two-body spin relaxation is provided. In some cases, because of nearby resonances, we can only provide an approximate lower bound on the resonance width.

| Atomic states $\lvert f,m_f\rangle \otimes \lvert f,m_f\rangle$ | $B_0$ (G) | $\Delta B$ (G) | $\mu_{\rm rel}$ ($\mu_{\rm B}$) | $a_{\rm bg}$ ($a_0$) | $r_{\rm e}$ ($a_0$) | Stability (G) |
|---|---|---|---|---|---|---|
| | | | $^6$Li-$^{85}$Rb | | | |
| $\lvert\frac{1}{2},\frac{1}{2}\rangle \otimes \lvert 2,2\rangle$ | 40.7 | >40 | 1.66 | −14.9 | <231 | ground state |
| $\lvert\frac{1}{2},-\frac{1}{2}\rangle \otimes \lvert 2,1\rangle$ | 402.5 | 27.3 | 1.58 | −14.9 | 358 | $\geqslant$149 |
| $\lvert\frac{1}{2},-\frac{1}{2}\rangle \otimes \lvert 2,0\rangle$ | 643.7 | 61.0 | 1.34 | −14.9 | 189 | $\geqslant$141 |
| $\lvert\frac{1}{2},-\frac{1}{2}\rangle \otimes \lvert 2,-1\rangle$ | 961.3 | 75.6 | 1.81 | −14.7 | 113 | $\geqslant$133 |
| $\lvert\frac{1}{2},-\frac{1}{2}\rangle \otimes \lvert 2,-2\rangle$ | 466.7 | >100 | 0.58 | −14.8 | <264 | $\geqslant$0 |
| | | | $^6$Li-$^{87}$Rb | | | |
| $\lvert\frac{1}{2},\frac{1}{2}\rangle \otimes \lvert 1,1\rangle$ | 1065.0 | 11.5 | 2.36 | −19.0 | 442 | ground state |
| $\lvert\frac{1}{2},-\frac{1}{2}\rangle \otimes \lvert 1,1\rangle$ | 1108.6 | 11.0 | 2.36 | −19.0 | 463 | $\geqslant$75 |

the reduced mass of the collision pair and $\mu_{\rm rel}$ is the difference in the magnetic moments of the closed channel (molecule) and the open-channel threshold. When this characteristic length scale is much smaller than, for example, the Fermi momentum wavelength, the resonance is considered broad [14]. In Table II, we present, based on calculations, the characteristics of seven large *s*-wave FRs in $^6$Li-$^{85}$Rb and $^6$Li-$^{87}$Rb mixtures stable with respect to two-body spin relaxation.

The *s*-wave scattering length for $^{85}$Rb-$^{85}$Rb collisions in each of the ground hyperfine sub-levels is negative except for at applied magnetic fields near one of the narrow homonuclear FRs, and none of these regions of positive scattering length overlaps with the $^6$Li-$^{85}$Rb FRs. Consequently, for the study of degenerate Fermi-Bose mixtures, the $^{85}$Rb Bose Einstein Condensate would only be metastable and of limited size near the heteronuclear FRs described here [31,32]. We also provide the characteristics of two broad resonances in $^6$Li-$^{87}$Rb mixtures where the *s*-wave scattering length for Rb is positive. These results are based on our previous analysis [27].

In summary, we have fully characterized the low-energy collisional properties of a mixture of $^6$Li and $^{85}$Rb atoms using FR spectroscopy. We interpret our experimental data using a full coupled-channels calculation and discuss seven broad heteronuclear FRs that are of importance for future experiments on Bose-Fermi mixtures realized in Li-Rb mixtures. This work presented here also provides data for further refinement of the Li-Rb interatomic potentials.

The authors acknowledge the support of the Canadian Institute for Advanced Research (CIfAR), the Natural Sciences and Engineering Research Council of Canada (NSERC), and the Canadian Foundation for Innovation (CFI)

[1] C. Chin, R. Grimm, P. Julienne, and E. Tiesinga, Rev. Mod. Phys. **82**, 1225 (2010).
[2] *Ultracold Fermi Gases, Proceedings of the International School of Physics "Enrico Fermi," Course CLXIV, Varenna, 2006*, edited by M. Inguscio, W. Ketterle, and C. Salomon (IOS Press, Amsterdam, 2008).
[3] M. W. Zwierlein, J. R. Abo-Shaeer, A. Schirotzek, C. H. Schunck, and W. Ketterle, Nature **435**, 1047 (2005).
[4] M. W. Zwierlein, A. Schirotzek, C. H. Schunck, and W. Ketterle, Science **311**, 492 (2006).
[5] G. B. Partridge, W. Li, R. I. Kamar, Y.-A. Liao, and R. G. Hulet, Science **311**, 503 (2006).
[6] E. Wille *et al.*, Phys. Rev. Lett. **100**, 053201 (2008).
[7] T. G. Tiecke, M. R. Goosen, A. Ludewig, S. D. Gensemer, S. Kraft, S. J. J. M. F. Kokkelmans, and J. T. M. Walraven, Phys. Rev. Lett. **104**, 053202 (2010).
[8] H. P. Büchler and G. Blatter, Phys. Rev. Lett. **91**, 130404 (2003).
[9] D. B. M. Dickerscheid, D. van Oosten, E. J. Tillema, and H. T. C. Stoof, Phys. Rev. Lett. **94**, 230404 (2005).
[10] F. M. Marchetti, C. J. M. Mathy, D. A. Huse, and M. M. Parish, Phys. Rev. B **78**, 134517 (2008).
[11] J. Zhang and H. Zhai, Phys. Rev. A **72**, 041602 (2005).
[12] M. Rizzi and A. Imambekov, Phys. Rev. A **77**, 023621 (2008).
[13] E. Fratini and P. Pieri, Phys. Rev. A **81**, 051605 (2010).
[14] M. Mashayekhi, J. Song, and F. Zhou, e-print arXiv:1003.3096v1.
[15] J. P. D'Incao and B. D. Esry, Phys. Rev. A **73**, 030703 (2006).
[16] J. G. Danzl, E. Haller, M. Gustavsson, M. J. Mark, R. Hart, N. Bouloufa, O. Dulieu, H. Ritsch, and H.-C. Nagerl, Science **321**, 1062 (2008).
[17] K.-K. Ni, S. Ospelkaus, M. H. G. de Miranda, A. Pe'er, B. Neyenhuis, J. J. Zirbel, S. Kotochigova, P. S. Julienne, D. S. Jin, and J. Ye, Science **322**, 231 (2008).
[18] A.-C. Voigt, M. Taglieber, L. Costa, T. Aoki, W. Wieser, T. W. Hänsch, and K. Dieckmann, Phys. Rev. Lett. **102**, 020405 (2009).
[19] M. Aymar and O. Dulieu, J. Chem. Phys. **122**, 204302 (2005).
[20] J. Doyle, B. Friedrich, R. Krems, and F. Masnou-Seeuws, Eur. Phys. J. D **31**, 149 (2004).
[21] R. V. Krems, Phys. Rev. Lett. **96**, 123202 (2006).
[22] Z. Li and R. V. Krems, Phys. Rev. A **75**, 032709 (2007).
[23] Z. Li and K. W. Madison, Phys. Rev. A **79**, 042711 (2009).
[24] C. Silber, S. Gunther, C. Marzok, B. Deh, Ph. W. Courteille, and C. Zimmermann, Phys. Rev. Lett. **95**, 170408 (2005).
[25] C. Marzok, B. Deh, Ph. W. Courteille, and C. Zimmermann, Phys. Rev. A **76**, 052704 (2007).
[26] B. Deh, C. Marzok, C. Zimmermann, and Ph. W. Courteille, Phys. Rev. A **77**, 010701 (2008).
[27] Z. Li, S. Singh, T. V. Tscherbul, and K. W. Madison, Phys. Rev. A **78**, 022710 (2008).
[28] C. Marzok, B. Deh, C. Zimmermann, Ph. W. Courteille, E. Tiemann, Y. V. Vanne, and A. Saenz, Phys. Rev. A **79**, 012717 (2009).
[29] K. Ladouceur, B. G. Klappauf, J. Van Dongen, N. Rauhut, B. Schuster, A. K. Mills, D. J. Jones, and K. W. Madison, J. Opt. Soc. Am. B **26**, 210 (2009).
[30] S. Chaudhuri, S. Roy, and C. Unnikrishnan, J. Phys.: Conf. Ser. **80**, 012036 (2007).
[31] C. C. Bradley, C. A. Sackett, J. J. Tollett, and R. G. Hulet, Phys. Rev. Lett. **75**, 1687 (1995).
[32] P. A. Ruprecht, M. J. Holland, K. Burnett, and M. Edwards, Phys. Rev. A **51**, 4704 (1995).